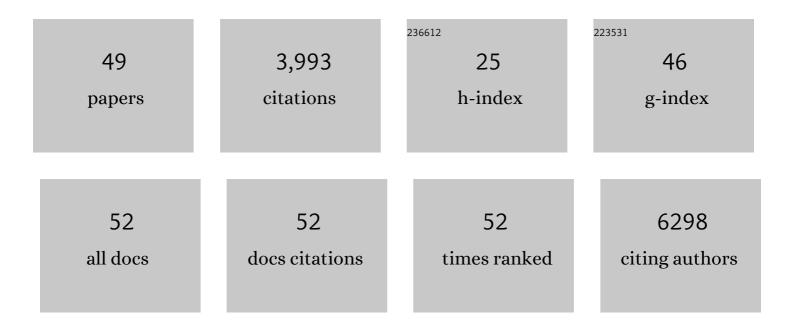
Trevor McKee

List of Publications by Year in descending order

Source: https://exaly.com/author-pdf/3446717/publications.pdf Version: 2024-02-01



#	Article	IF	CITATIONS
1	Dynamic imaging of collagen and its modulation in tumors in vivo using second-harmonic generation. Nature Medicine, 2003, 9, 796-800.	15.2	798
2	Role of tumor-host interactions in interstitial diffusion of macromolecules: Cranial vs. subcutaneous tumors. Proceedings of the National Academy of Sciences of the United States of America, 2001, 98, 4628-4633.	3.3	529
3	Diffusion and Convection in Collagen Gels: Implications for Transport in the Tumor Interstitium. Biophysical Journal, 2002, 83, 1650-1660.	0.2	457
4	Degradation of Fibrillar Collagen in a Human Melanoma Xenograft Improves the Efficacy of an Oncolytic Herpes Simplex Virus Vector. Cancer Research, 2006, 66, 2509-2513.	0.4	363
5	Reprogramming Metabolism with Metformin Improves Tumor Oxygenation and Radiotherapy Response. Clinical Cancer Research, 2013, 19, 6741-6750.	3.2	268
6	Two-photon fluorescence correlation microscopy reveals the two-phase nature of transport in tumors. Nature Medicine, 2004, 10, 203-207.	15.2	163
7	GLUT1 inhibition blocks growth of RB1-positive triple negative breast cancer. Nature Communications, 2020, 11, 4205.	5.8	130
8	In vivo imaging of extracellular matrix remodeling by tumor-associated fibroblasts. Nature Methods, 2009, 6, 143-145.	9.0	120
9	Prkar1a is an osteosarcoma tumor suppressor that defines a molecular subclass in mice. Journal of Clinical Investigation, 2010, 120, 3310-3325.	3.9	89
10	Mice with Tissue Inhibitor of Metalloproteinases 4 (Timp4) Deletion Succumb to Induced Myocardial Infarction but Not to Cardiac Pressure Overload. Journal of Biological Chemistry, 2010, 285, 24487-24493.	1.6	80
11	Solid stress facilitates spheroid formation: potential involvement of hyaluronan. British Journal of Cancer, 2002, 86, 947-953.	2.9	69
12	Towards extracellular matrix normalization for improved treatment of solid tumors. Theranostics, 2020, 10, 1960-1980.	4.6	68
13	RANKL blockade prevents and treats aggressive osteosarcomas. Science Translational Medicine, 2015, 7, 317ra197.	5.8	67
14	Cross-species genomics identifies DLG2 as a tumor suppressor in osteosarcoma. Oncogene, 2019, 38, 291-298.	2.6	65
15	Multiplexed imaging of immune cells in staged multiple sclerosis lesions by mass cytometry. ELife, 2019, 8, .	2.8	56
16	Radiation and Heat Improve the Delivery and Efficacy of Nanotherapeutics by Modulating Intratumoral Fluid Dynamics. ACS Nano, 2018, 12, 7583-7600.	7.3	55
17	Lack of Telopeptides in Fibrillar Collagen I Promotes the Invasion of a Metastatic Breast Tumor Cell Line. Cancer Research, 2005, 65, 5674-5682.	0.4	50
18	Evofosfamide for the treatment of human papillomavirus-negative head and neck squamous cell carcinoma. JCI Insight, 2018, 3, .	2.3	44

TREVOR MCKEE

#	Article	IF	CITATIONS
19	Acute Kidney Injury in Severe COVID-19 Has Similarities to Sepsis-Associated Kidney Injury. Mayo Clinic Proceedings, 2021, 96, 2561-2575.	1.4	41
20	A Progesterone-CXCR4 Axis Controls Mammary Progenitor Cell Fate in the Adult Gland. Stem Cell Reports, 2015, 4, 313-322.	2.3	38
21	Isotopologous Organotellurium Probes Reveal Dynamic Hypoxia In Vivo with Cellular Resolution. Angewandte Chemie - International Edition, 2016, 55, 13159-13163.	7.2	32
22	Irradiation reduces interstitial fluid transport and increases the collagen content in tumors. Clinical Cancer Research, 2003, 9, 5508-13.	3.2	32
23	Resistance to dual blockade of the kinases PI3K and mTOR in <i>KRAS</i> -mutant colorectal cancer models results in combined sensitivity to inhibition of the receptor tyrosine kinase EGFR. Science Signaling, 2014, 7, ra107.	1.6	30
24	Quantitative Visualization of Hypoxia and Proliferation Gradients Within Histological Tissue Sections. Frontiers in Bioengineering and Biotechnology, 2019, 7, 397.	2.0	28
25	Prognostic influence of tumor microenvironment after hypofractionated radiation and surgery for mesothelioma. Journal of Thoracic and Cardiovascular Surgery, 2020, 159, 2082-2091.e1.	0.4	28
26	MATE2 Expression Is Associated with Cancer Cell Response to Metformin. PLoS ONE, 2016, 11, e0165214.	1.1	25
27	The mTOR Targets 4E-BP1/2 Restrain Tumor Growth and Promote Hypoxia Tolerance in PTEN-driven Prostate Cancer. Molecular Cancer Research, 2018, 16, 682-695.	1.5	24
28	Evaluation of optimal biopsy location for assessment of histological activity, transcriptomic and immunohistochemical analyses in patients with active Crohn's disease. Alimentary Pharmacology and Therapeutics, 2019, 49, 1401-1409.	1.9	21
29	Administration of Hypoxia-Activated Prodrug Evofosfamide after Conventional Adjuvant Therapy Enhances Therapeutic Outcome and Targets Cancer-Initiating Cells in Preclinical Models of Colorectal Cancer. Clinical Cancer Research, 2018, 24, 2116-2127.	3.2	20
30	Role of chemokines in metastatic niche: new insights along with a diagnostic and prognostic approach. Apmis, 2018, 126, 359-370.	0.9	19
31	Thermosensitive liposomal cisplatin in combination with local hyperthermia results in tumor growth delay and changes in tumor microenvironment in xenograft models of lung carcinoma [*] . Journal of Drug Targeting, 2016, 24, 865-877.	2.1	18
32	Variations in the Abundance of Lipid Biomarker lons in Mass Spectrometry Images Correlate to Tissue Density. Analytical Chemistry, 2016, 88, 12099-12107.	3.2	16
33	Metalloprotease inhibitor TIMP proteins control FGF-2 bioavailability and regulate skeletal growth. Journal of Cell Biology, 2019, 218, 3134-3152.	2.3	16
34	Correlation of Somatostatin Receptor-2 Expression with Gallium-68-DOTA-TATE Uptake in Neuroblastoma Xenograft Models. Contrast Media and Molecular Imaging, 2017, 2017, 1-10.	0.4	15
35	Identification of RSK and TTK as Modulators of Blood Vessel Morphogenesis Using an Embryonic Stem Cell-Based Vascular Differentiation Assay. Stem Cell Reports, 2016, 7, 787-801.	2.3	14
36	Nanoparticle Formulation Derived from Carboxymethyl Cellulose, Polyethylene Glycol, and Cabazitaxel for Chemotherapy Delivery to the Brain. Bioconjugate Chemistry, 2018, 29, 2009-2020.	1.8	14

TREVOR MCKEE

#	Article	IF	CITATIONS
37	Computationally-Guided Development of a Stromal Inflammation Histologic Biomarker in Lung Squamous Cell Carcinoma. Scientific Reports, 2018, 8, 3941.	1.6	11
38	Discoidin domain receptor 1-deletion ameliorates fibrosis and promotes adipose tissue beiging, brown fat activity, and increased metabolic rate in a mouse model of cardiometabolic disease. Molecular Metabolism, 2020, 39, 101006.	3.0	10
39	Neoadjuvant olaparib targets hypoxia to improve radioresponse in a homologous recombination-proficient breast cancer model. Oncotarget, 2017, 8, 87638-87646.	0.8	10
40	Isotopologous Organotellurium Probes Reveal Dynamic Hypoxia In Vivo with Cellular Resolution. Angewandte Chemie, 2016, 128, 13353-13357.	1.6	9
41	Pentraxin 3 deficiency enhances features of chronic rejection in a mouse orthotopic lung transplantation model. Oncotarget, 2018, 9, 8489-8501.	0.8	9
42	The expression of CD markers in solid tumors: Significance in metastasis and prognostic value. Histology and Histopathology, 2018, 33, 1005-1012.	0.5	9
43	Blocking the GITR-GITRL pathway to overcome resistance to therapy in sarcomatoid malignant pleural mesothelioma. Communications Biology, 2021, 4, 914.	2.0	7
44	Tracking adiponectin biodistribution via fluorescence molecular tomography indicates increased vascular permeability after streptozotocin-induced diabetes. American Journal of Physiology - Endocrinology and Metabolism, 2019, 317, E760-E772.	1.8	5
45	Heterogeneity of Circulating Tumor Cell–Associated Genomic Gains in Breast Cancer and Its Association with the Host Immune Response. Cancer Research, 2021, 81, 6196-6206.	0.4	5
46	QUANTIFYING NANOPARTICLE TRANSPORT <i>IN VIVO</i> USING HYPERSPECTRAL IMAGING WITH A DORSAL SKINFOLD WINDOW CHAMBER. Journal of Innovative Optical Health Sciences, 2012, 05, 1250023.	0.5	4
47	SP-0337: Understanding and targeting the underlying drivers of tumor hypoxia. Radiotherapy and Oncology, 2018, 127, S178.	0.3	0
48	A Phase 2 biomarker-enriched study of evofosfamide (TH-302) in patients with advanced melanoma Journal of Clinical Oncology, 2015, 33, TPS9089-TPS9089.	0.8	0
49	Development and Validation of a Digital Analysis Method to Quantify CD3-immunostained T Lymphocytes in Whole Slide Images of Crohn's Disease Biopsies. Applied Immunohistochemistry and Molecular Morphology, 2022, Publish Ahead of Print, .	0.6	0